Published online 8 November 2013 *Nucleic Acids Research, 2014, Vol. 42, No. 3* ***1593–1605***
doi:10.1093/nar/gkt1090

Redox-active quinones induces genome-wide DNA methylation changes by an iron-mediated and Tet-dependent mechanism

Bailin Zhao[1], Ying Yang[2], Xiaoli Wang[1], Zechen Chong[2], Ruichuan Yin[1], Shu-Hui Song[2], Chao Zhao[1], Cuiping Li[1], Hua Huang[1], Bao-Fa Sun[2], Danni Wu[1], Kang-Xuan Jin[2], Maoyong Song[1], Ben-Zhan Zhu[1], Guibin Jiang[1], Jannie M. Rendtlew Danielsen[2,3], Guo-Liang Xu[4], Yun-Gui Yang[2,*] and Hailin Wang[1,*]

[1]State Key Laboratory of Environmental Chemistry and Ecotoxicology, Research Center for Eco-Environmental Sciences, Chinese Academy of Sciences, Beijing 100085, China, [2]Disease Genomics and Individualized Medicine Laboratory, Beijing Institute of Genomics, Chinese Academy of Sciences, Beijing 100101, China, [3]The Novo Nordisk Foundation Center for Protein Research, Ubiquitin Signalling Group, Faculty of Health Sciences, Blegdamsvej 3b, 2200, Copenhagen, Denmark and [4]Group of DNA Metabolism, The State Key Laboratory of Molecular Biology, Institute of Biochemistry and Cell Biology, Shanghai Institutes for Biological Sciences, Chinese Academy of Sciences, Shanghai 200031, China

Received September 14, 2013; Revised October 12, 2013; Accepted October 16, 2013

ABSTRACT

DNA methylation has been proven to be a critical epigenetic mark important for various cellular processes. Here, we report that redox-active quinones, a ubiquitous class of chemicals found in natural products, cancer therapeutics and environment, stimulate the conversion of 5mC to 5hmC *in vivo*, and increase 5hmC in 5751 genes in cells. 5hmC increase is associated with significantly altered gene expression of 3414 genes. Interestingly, in quinone-treated cells, labile iron-sensitive protein ferritin light chain showed a significant increase at both mRNA and protein levels indicating a role of iron regulation in stimulating Tet-mediated 5mC oxidation. Consistently, the deprivation of cellular labile iron using specific chelator blocked the 5hmC increase, and a delivery of labile iron increased the 5hmC level. Moreover, both *Tet1*/*Tet2* knockout and dimethyloxalylglycine-induced Tet inhibition diminished the 5hmC increase. These results suggest an iron-regulated Tet-dependent DNA demethylation mechanism mediated by redox-active biomolecules.

INTRODUCTION

DNA methylation regulates gene expression and renders cellular identity, and also is critically involved in genome imprinting, inactivation of X chromosome and parasite elements, and documentation of epigenetic memory (1). The 5-methylcytosine (5mC) could be oxidized by the ten-eleven translocation (TET) family of hydroxylases to the sixth DNA base 5-hydroxymethylcytosine (5hmC) (2–6). Varying degrees of the 5hmC modification has been found in several tissue types (3,7,8). Genome-wide mapping analysis has shown a strong enrichment of 5hmC within exons and near transcription start sites (TSSs), pointing to a potential role in transcriptional regulation (9–11). Furthermore, impaired hydroxylation of 5mC has been observed in myelodysplastic syndromes and several forms of myeloid leukemias (12,13).

Currently, the generation of 5hmC in mammalian cells is primarily attributed to enzymatic oxidation of 5mC by either of the three existing TET proteins (4–6,14). The generated 5hmC could be further converted to removable 5-formylcytosine and 5-carboxycytosine by further oxidation, providing a mechanism for active DNA demethylation (5,6). Interestingly, small biomolecules can alter the epigenetic DNA methylation patterns and regulate life processes (14), even cause some diseases like

*To whom correspondence should be addressed. Tel: +86 10 62849600; Fax: +86 10 62849600; Email: hlwang@rcees.ac.cn
Correspondence may also be addressed to Yun-Gui Yang. Tel: +86 01 82997642; Fax: +86 01 82997642; Email: ygyang@big.ac.cn

The authors wish it to be known that, in their opinion, the first three authors should be regarded as Joint First Authors.

cancer (15–18). These xenobiotics include metals (19–21), vitamin C (14), endocrine-disrupting chemicals (22) and some persistent organic pollutants (23,24). On the other hand, the alteration of epigenetic states including DNA methylome could be exploited to treat cancers (25). However, little is known about the effects of small biomolecules on Tet-mediated DNA demethylation.

Since the oxidation of 5mC catalyzed by Tet proteins is assisted with some small cofactors, e.g., iron (II) and α-ketoglutarate (4–6), the catalytic activity of Tet proteins should be affected by the levels of iron (II) and α-ketoglutarate in mammalian cells. The cellular levels of iron (II) and α-ketoglutarate are altered by cellular milieu, in particular redox status (26–30). Quinones are a ubiquitous class of redox-active compounds found in natural products, cancer therapeutics, endogenous biochemical, and environment pollutants or generated through metabolism of hydroquinones and/or catechols (31). We speculate that redox-active quinones may change the hemostasis of iron or α-ketoglutarate, therefore influence the catalytic activity of Tet dioxygenases. Since Tet dioxygenses mediate the oxidation of 5mC and initiate passive and active DNA demthylation (5,6), it expects that quinones may alter DNA demethylation process through changing Tet oxidation activity. Here, we tested if quinones could impact the conversion of 5mC to 5hmC at cellular levels. If so, we would characterize the possible roles of those compounds in modulating DNA demethylation and investigate the underlying mechanism.

MATERIALS AND METHODS

Cell culture and treatment

Human fetal lung fibroblast cell line MRC-5, human lung adenocarcinoma cell line A549 and hepatocellular carcinoma cell line HepG2 (supplied by cell culture center, Institute of Basic Medical Sciences, Chinese Academy of Medical Sciences, Beijing, China) were cultured in Dulbecco's modified Eagle's medium (DMEM) with high glucose medium and in RPMI 1640 medium, respectively, in 5% CO_2 at 37°C, both of which contained 10% fetal bovine serum, 100 U/ml penicillin, 100 μg/ml streptomycin. The wild type (WT) and *Tet1* and *Tet2* genes knocked out (*Tet1*/*Tet2*$^{-/-}$) mouse embryo stem cell were maintained in DMEM medium (HyClone, Thermo Fisher Scientific Inc., MA, USA) supplemented with 20% ES FBS (Gibco, Life Technologies Corporation., Grand Island, NY, USA), 0.1 mM non-essential amino acids, 2 mM L-glutamine, 0.1 mM β-mercaptoethanol, 1000 U/ml leukemia inhibitory factor (LIF) (Millipore, Billerica, MA, USA), 1.0 μM PD 0325901 (Stemgent, Cambridge, MA, USA) and 3.0 μM CHIR 99021 (Stemgent, Cambridge, MA, USA). For all experiments, mES cells were trypsinized and plated in culture dishes pretreated with 0.1% gelatin, then incubated in a humidified 37°C incubator supplied with 5% CO_2. For the generation of 5hmC in cells, MRC-5 or mES cells were treated with 20 μM or 50 μM tetrachloro-1,4-benzoquinone (TCBQ) or tetrachloro-1,4-hydroquinone (TCHQ) for 24 h. For the effect of dimethyloxaloylglycine (DMOG) on TCBQ-dependent generation of 5hmC, A549 cells were treated by 50 μM TCBQ or 200 μM DMOG or both for 24 h. For the dose-dependent assay, A549 cells (5×10^5 cells) were seeded in culture medium for 24 h and then treated with 0, 1, 5, 20 and 50 μM of TCBQ or TCHQ for 24 h. The medium was removed and the cells were washed three times with phosphate buffered saline (PBS), and fresh medium containing the same concentration of TCBQ or TCHQ added. The treatment was consecutively repeated three times over a total period of 72 h. To determine the effect of exposure time on the level of 5hmC, A549 cells were treated with 50 μM TCBQ or TCHQ for 0, 6, 12, 24 and 48 h (two 24 h treatments), 72 h (three 24 h treatments). In order to elucidate the repair mechanism of 5hmC in A549 cells, after being treated with 50 μM TCBQ for 72 h as described above, the TCBQ-containing medium was removed and the cells were washed three times with PBS. TCBQ-treated A549 cells were then recultured in fresh medium without chemical for 0, 12, 24, 48, 72 and 96 h. HepG2 cells were treated with TCBQ (20 μM) and TCHQ (50 μM) for 72 h and the treatment was carried out as described above. In all, 50 μM of tetrabromo-1,4-benzoquinone (TBrBQ), 2,5-dichloro-1,4-benzoquinone (2,5-DCBQ), 2,6-dichloro-1,4-benzoquinone (2,6-DCBQ), 2-chloro-1,4-benzoquinone (2-CBQ), O-chloranil and 2-methyl-1,4-benzoquinone (2-MBQ) were also used in A549 cells exposure experiments for 24 h. All the cultured cells treated with chemicals were harvested for further analysis, and the exposure experiments were repeated three times.

DNA extraction and enzymatic digestion

Genomic DNA was extracted from the harvested cells using a Genomic DNA Purification Kit (Promega, Madison, WI, USA) according to the manufacturer's instructions. To prevent artificial oxidative damage to DNA, 0.1 mM DFO was added in the processes of DNA extraction and purification (32). The concentration and quality of the extracted DNA were evaluated by measuring the absorbance at 260 nm and 280 nm.

The DNA (5 μg) was digested with 1 U DNase I, 2 U calf intestinal phosphatase and 0.005 U snake venom phosphodiesterase I (New England Biolabs, Ipswich, MA, USA) at 37°C for 24 h. A total of 1 mM DFO was used during the enzymatic digestion of DNA (32). Proteins from the DNA digestion system were removed prior to the UHPLC-MS/MS analysis, using Microcon centrifugal filter device (Millipore, Bedford, MA, USA) with the 3000 D cutoff membrane by centrifuging at 10 000 g for 1 h.

UHPLC-MRM MS/MS analysis

The Agilent 1200 Series Rapid Resolution LC system and a reverse-phase Zorbax SB-C18 2.1 × 100 mm column (1.8 μm particles) were applied in the UHPLC analysis. The method was same as recently described (14) or with a minor modification. In brief, the digested DNA (5.0–15.0 μl) was injected onto the column and nucleosides separation was completed using the mobile phase of 95% water (containing 0.1% formic acid) and 5.0% methanol at

a flow rate of 0.3 ml/min, or a gradient elution was used for separation: 0–3 min, 5.0% B; 3–6 min, 15.0% B; 6–10 min, 100% B; 10–15 min, 5.0% B. Solvent A was an aqueous solution of 2.0 mM NH_4HCO_3 (pH 9.0), and solvent B was 100% methanol, the flow-rate was 0.25 ml/min. Mass spectrometric detection was achieved by the Agilent (Santa Clara, CA, USA) 6410B Triple Quadrupole mass spectrometer with an electrospray ionization source. Positive ionization mode, 3500 V capillary voltage as well as 300°C and 9 l/min nitrogen drying gas were selected for the experiment. For nucleotides analysis, the fragmentor voltage and collision energy were performed at 90 V and 5 eV, respectively, with a scan time of 100 ms. Multiple reaction monitoring (MRM) mode was used for the LC-MS/MS analysis. 5hmC in cellular DNA was detected in the form of the mononucleoside 5hmdC by monitoring the transitions of m/z 258.1 → 142.1. The amount of 5hmC was calibrated by standard curve.

Dot blot for 5hmC analysis

Briefly, DNA samples were diluted with 10 mM Tris–HCl, pH 8.0, and denatured by heating at 95°C for 10 min, and chilled on ice for 5 min. Then the DNA samples were loaded on Amersham Hybond N+ membrane (GE Healthcare) using a 96-well dot-blot apparatus (Bio-Rad). After being baked in 80°C for 2 h and blocked by 5% non-fat milk for 1 h at room temperature, the membrane was incubated with a polyclonal anti-5-hmC antibody (Active Motif 39791, 1:10,000) at 4°C overnight. 5-hmC was visualized by using chemiluminescence after being incubated with secondary antibody against rabbit (Roch, 1: 8000) for 30 min at room temperature. 5hmC standard (active motif) at 1, 0.5, 0.25 ng from top to bottom was used as positive control.

Western blot analysis

Cytoplasmic and nucleic extracts from MRC-5 cells treated by 20 μM TCBQ or 0.02% (v/v) DMSO were prepared with NE-PER® Nuclear and Cytoplasmic Extraction Reagents (Thermo Scientific) according to the manufacturer's instructions. Protein concentrations were measured using the Bradford Assay, and 60 μg protein extracts were separated on a 12% sodium dodecyl sulfate–polyacrylamide gel electrophoresis. Then proteins were transferred to a nitrocellulose membrane, blocked with 5% non-fat milk and incubated overnight at 4°C with antibodies against the light chain of ferritin (FTL) (abcam, 1:500), ferroportin (Fpn) (sigma, 1:1000), GAPDH (Sigma, 1:1000). Blots were incubated with secondary antibody against mouse (1:8000) and rabbit (1: 8000) for 1 h before visualization. Cytoplasmic and nucleic extracts from MRC-5 cells treated with 100 μM ferric nitrilotriacetate (Fe-NTA) were applied for positive control.

5hmC pull-down, deep sequencing and data analysis

Genomic DNA from TCBQ or Control DMSO treated MRC-5 cells was purified by using Wizard genomic DNA purification kit (Promega) according to the manufacturer's instructions. Genomic DNA samples were further sonicated into short fragments (about 300 bp) by using Covaris DNA shearing (Covaris S2 SonoLAB Single) with microTUBEs according to the manufacturer's instructions. Sonicated DNA was then purified with phenol/chloroform/isoamyl alcohol (25:24:1) precipitation. 5hmC was pulled down as described previously (11). After purification, 10 ng of the pull-downed 5hmC containing DNA was end-repaired, adenylated, ligated to adapters and single-end sequenced on a HiSeq 2000 system (Illumina) according to the manufacturer's recommendations for Illumina ChIP-Seq to identify peak enrichment. To the 101-bp sequence reads, as a subset of reads may contain all or part of the adaptor oligonucleotide sequence, a custom pairwise alignment script was applied to find reads hit by adaptor sequence, which required at least five bases match from the beginning of the adaptor, and at least 90% similarity. If detected, the read was trimmed to the preceding base. Low-quality base trimming was performed by Trimmomatic (http://www.usadellab.org/cms/index.php?page=trimmomatic) with default parameters. Clean reads were mapped to the *Homo sapiens* reference genome (Hm19) using BWA (33) with default parameters. The maximum number of mismatches allowed was 3. To the reads mapped to different genome locations with the same quality of mapping, we randomly chose one location. The 5hmC peaks were analyzed using MACS (34). By default, MACS retains no more than one read on the same starting position in the genome, which can removes redundant reads. Peak enrichment with a linear normalization were implemented in MACS. Genes with fold change over 5 were selected for GO and KEGG analysis. The metagene analysis of the 5hmC peaks were performed by CEAS package (33,34) (http://liulab.dfci.harvard.edu/CEAS/).

RNA-seq

Total RNA was isolated from TCBQ treated and DMSO treated MRC-5 cells using RNAzol (Molecular Research Center, Inc.). Poly(A) RNA from 1 μg of total RNA was used to generate the cDNA library according to TruSeq RNA Sample Prep Kit protocol which was then be sequenced using the Illumina system. Since we sequenced single-end 101 bp reads, we kept a caution avoiding removing duplicates for that may introduce biases in the expression analysis. We aligned those high-quality reads to the masked *Homo sapiens* reference genome (hg19) and junction sequences using BWA 0.5.8 software (35) allowing up to four mismatches. All the uniquely mapped reads were used to define gene expression level based on our developed method (36). We modified the RPKM (measured in reads per kilobase of exon per million mapped sequence reads, which is a normalized measure of exonic read density) calculation described by Mortazavi *et al.* (37) to include junction fragments. By including reads that map to junction fragments, we ensure that genes with many introns are not underrepresented in the RPKM estimate. To examine differential expression, we used a MARS (MA-plot-based method with Random Sampling model) method to identify

differentially expressed genes which was described in DNAseq (38). To determine the DEGs, the *P*-value and FDR-adjusted *P*-value (using both Benjamini-Hochberg correction (39) and the method of Storey and Tibshirani (40)) were both considered: $P < 0.001$ and $q < 0.05$ (indeed both q-values < 0.003).

Gene ontology and enrichment analysis

Gene ontology (GO) analysis of differentially expressed genes was performed using DAVID (http://david.abcc.ncifcrf.gov/). An enrichment map of 5hmC enriched genes or overlapped genes from 5hmC-seq and differentially expressed genes was generated by using the Cytoscape (Ver. 2.8.2) installed with Enrichment Map plugin. Red node represents each enriched GO pathway. Node size equals the total number of genes in each GO pathway. Edge thickness is in proportion to the number of overlapped genes between nodes. GO pathways of related functions are sorted into one cluster, marked with circles and labels. Gene numbers in each cluster are also labeled.

Verification of 5hmC-enriched regions with boronic acid method

Genomic DNA purified from TCBQ or DMSO treated MRC-5 cells was glucosylated with the EpiMark™ 5hmC and 5mC Analysis Kit (NEB, Ipswich, MA, USA) according to the manufacturer's instructions with minor modification. For 5hmC-enriched regions verification, genomic DNA with glucosylation or not was treated by 5 mM boronic acid (BA) reagent in 100 mM Na_2HPO_4 (pH 8.5) and 50 mM NaCl buffer, then the treated DNA was diluted to 10 ng/μl and 1 μl was used in the 25 μl RT-qPCR reaction containing 1×GoTaq® SYBR Green qPCR Master Mix (Promega, Madison, WI, USA) and 0.2 μM forward and reverse primers. qPCR was performed on a Mx3500P Real-time PCR system (Stratagene) and the cycling condition was as follows: 95°C for 2 min and then 40 cycles of PCR at 95°C for 15 s, 57°C for 15 s and 25°C for 60 s. The experiments were independently performed triplicate. The primer pairs used for detection of 5hmC-enriched regions were listed in Supplementary Table S4.

RNA isolation, cDNA synthesis and quantitative real-time PCR

MRC-5 cells were treated with 20 μM TCBQ dissolved in DMSO solution or DMSO solution only. Cells were trypsinized routinely after 24 h treatment. Total RNA was extracted using TRI® Reagent (Sigma) (Invitrogen). cDNA was synthesized by RevertAid™ First Strand cDNA Synthesis Kit with Oligo dT primers (Fermentas, K1622) following the manufacturer's recommendations. PCRs were carried out on a 7500 Real-time PCR system (Applied Biosystems) in 25 μl reaction volume containing 1 μl cDNA, 2X SYBR Green PCR Master Mix (TAKARA) and 200 nM primers. All samples were analyzed by RT-qPCR for three times. The primer pairs used for detection of transcripts were listed in Supplementary Table S5.

Statistical analysis

The *t*-test using two-way ANOVA in Grouped Analyses of Prism5 software was applied for statistical analysis.

RESULTS

The conversion of 5mC to 5hmC by redox-active quinones *in vivo*

To test whether redox-active quinones could influence the formation of 5hmC *in vivo*, we treated MRC-5 cells with TCBQ of 20 μM. TCBQ, as one example of halogenated quinoid compounds, is a reactive metabolite of the widely used biocide pentachlorophenol (PCP) (41,42), which has been classified as a Group 2B compounds (possible carcinogen to human) by IARC (43). Moreover, TCBQ analogs have been recently identified as toxic disinfection byproducts in drinking water (44). By coupling ultra-high performance liquid chromatography-triple quadrupole mass spectrometry with multiple-reaction monitoring (UHPLC-MRM-QQQ), we were able to detect trace amounts of cellular 5hmC (Supplementary Figure S1). Indeed, TCBQ treatment increased the level of 5hmC by ~1.9-fold compared to the DMSO control (from 25.8 per million C to 48.8 per million C) (Figure 1A and B). Furthermore, TCHQ (20 μM), the reduced form of TCBQ, could also induce 5hmC formation (Figure 1A and B). An anti-5hmC antibody-based dot-blot analysis further confirmed the increase of 5hmC induced by 20 μM TCBQ- or TCHQ-treatment while the uploaded amounts of genomic DNA were same as indicated by methyl blue staining (Figure 1C). The increase of 5hmC observed after TCBQ- or TCHQ-treatment was both dose (0–50 μM) and time (0–72 h) dependent (Supplementary Figure S2A–D). The level of 5hmC in TCBQ- or TCHQ-treated cells increases over 3 days of exposure, indicating that the generated 5hmC is stable and accumulates in cells. The generated 5hmC by 72-h TCBQ exposure could not be removed within 96 h after the TCBQ was completely withdrawn from the culture (Supplementary Figure S2E), supporting the accumulation and persistence of TCBQ-induced 5hmC. The TCBQ/TCHQ-induced formation of 5hmC was also detected in human A549 cells and HepG2 cells (Supplementary Figure S2A, S2C and S2F).

TCBQ and TCHQ tested here are reactive metabolites of PCP, which has been found in body fluids (plasma or urine) of non-occupationally exposed individuals (0–7.0 μM) and in the blood of occupationally exposed workers (22.5–170 μM) (42,45). Since >20% of PCP could be converted to TCHQ and TCBQ (46), the total concentration of TCBQ and TCHQ is estimated about 0–1.5 μM for non-occupationally exposed individuals and 4.5–34 μM for occupationally exposed individuals. Here we demonstrated that the cells treated by TCHQ at 1.0 μM could significantly increase the level of 5hmC (Supplementary Figure S2C). The tested doses of TCBQ and TCHQ here are comparable to that of non-occupational exposure and are even lower than that for occupational exposure. These results clearly suggest that the observed effects of TCBQ and TCHQ on cellular processes by 5hmC are physiologically relevant.

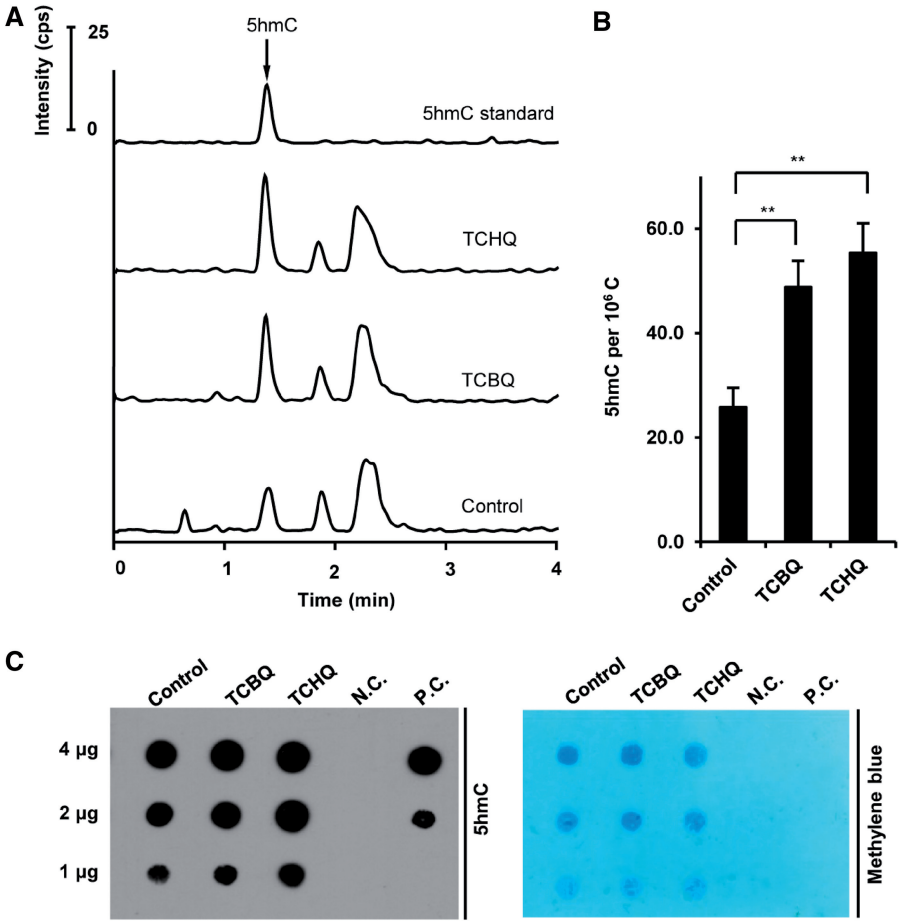

Figure 1. The conversion of 5mC to 5hmC by redox-active quinones at cellular level. (**A** and **B**) UHPLC-MRM MS/MS analysis (A) and quantitation (B) of 5hmC in the enzymatic digest of genomic DNA from MRC-5 cells. The cells were treated with 20 μM TCBQ or TCHQ. The peak corresponding to 5hmC is denoted by the arrow, and the other two peaks are un-identified. (**C**) Immunodotblotting analysis of 5hmC in MRC-5 cells upon 20 μM TCBQ- or TCHQ-treatment (left panel). The amount of uploaded DNA samples was indicated by methyl blue staining (right panel). N.C and P.C. represent negative and positive control, respectively. Control genomic DNA was extracted from the cells only treated with the solvent DMSO (0.02%, v/v) with the same amount as that used in TCBQ/TCHQ treatment. $^{**}P < 0.01$, determined using Student's *t*-test, two-tailed. Error bars, mean ± S.E.M. for triplicate experiments.

The formation of 5hmC stimulated by quinone is Tet dependent

Since quinones are redox active (31), TCBQ may stimulate the formation of highly reactive oxygen species (ROS). Indeed, a significant increase in highly reactive ROS was observed in TCBQ-treated cells as measured by 2′,7′-dihydroxychlorofluorescein diacetate (DCFH-DA) fluorescence method (47) (Supplementary Figure S3). The production of highly reactive ROS was dependent on TCBQ concentration (Supplementary Figure S3C), and the treatment with 50 μM TCBQ increased the average fluorescent intensity 25-fold above control level after 2 h (Supplementary Figure S3C). It is not known whether the elevated ROS can directly react with genomic DNA as a type of chemical reaction (48,49) or indirectly stimulate the enzymatically catalytic reaction enhancing 5hmC formation. So, we first tested whether the generation of 5hmC is pertinent to TET family dioxygenases, which are enzymatically associated with 5mC oxidation and resultant 5hmC formation (2–6). We measured 5hmC in the Tet-proficient mouse embryonic stem (ES) cells treated with TCBQ or TCHQ. Without TCBQ/TCHQ treatment, the frequency of 5hmC in genomic DNA of ES cells is estimated as 7.39×10^2 per million C, which is about 30 times higher than that of MRC-5 cells. This indicates a much higher oxidation activity of Tet proteins in mouse ES cells. Treatment with 20 μM TCBQ or TCHQ over 24 h increased the level of 5hmC to 1.57×10^3 and 1.75×10^3 per million C, respectively (Figure 2A and B). Evidently, the generation of 5hmC stimulated by quinones increases with an increased Tet oxidation activity, suggesting a linkage of quinone-stimulation effect with Tet oxidation activity. By double knockout of *Tet1*/*Tet2* (*Tet1*/*Tet2*$^{-/-}$) in mouse ES cells, 5hmC was barely detectable even after TCBQ- or TCHQ-treatment (Figure 2A and B). These results clearly support that the formation of 5hmC by quinones requires Tet1 or Tet2 proteins, rather than a direct reaction of highly reactive ROS with genomic DNA. Moreover, dimethyloxalylglycine (DMOG), a cell-permeable competitor of α-ketoglutarate (50), inhibited

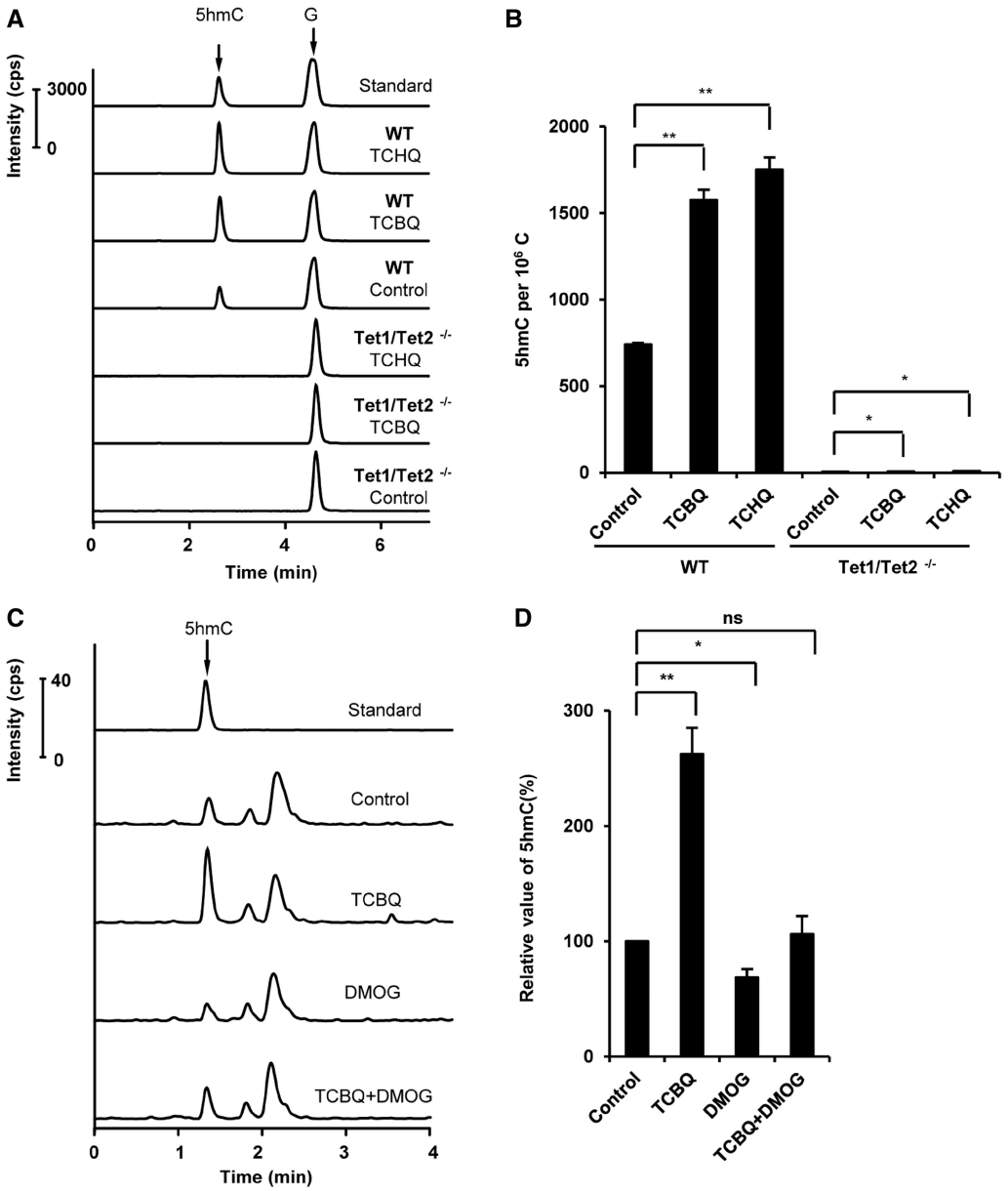

Figure 2. TET-dependent generation of 5hmC by redox-active quinones in cells. (**A** and **B**) UHPLC-MRM MS/MS analysis (A) and quantitation (B) of 5hmC in the enzymatic digest of genomic DNA from wild type (WT) and *Tet1*/*Tet2* double knock-out (*Tet1*/*Tet2*$^{-/-}$) mouse ES cells treated by 20 μM TCBQ or TCHQ. (**C** and **D**) UHPLC-MRM MS/MS analysis (C) and quantitation (D) of 5hmC in genomic DNA from 50 μM TCBQ-treated A549 cells in the absence or presence of 200 μM DMOG. Control DNA was extracted from cells treated with 0.02% (v/v) DMSO. *$P < 0.05$, **$P < 0.01$, determined using Student's *t*-test, two-tailed. Error bars, mean ± S.E.M. for triplicate experiments.

the 5hmC formation in TCBQ-treated MRC-5 cells (Figure 2C and D). Together, the above results consistently support the involvement of Tet proteins in quinones-stimulated generation of 5hmC *in vivo*.

The quinone stimulation of Tet oxidation activity is associated with iron regulation *in vivo*

The next question we asked is how quinones stimulate the 5mC oxidation activity of Tet proteins. Since certain ROS could elevate the labile iron as reported previously (26–29), we speculated that ROS induced by TCBQ treatment might stimulate the catalytic activity of Tet proteins by increasing the availability of its cofactor iron (II) at cellular level. Interestingly, we observed an elevation of the light chain of ferritin (a major iron-storage protein at the cellular and organismal level) in TCBQ-treated MRC-5 at both levels of mRNA and protein (Figures 3A and 7C). Essentially, both the levels of cytoplasmic and nuclear ferritin light chain (FTL) were up-regulated upon TCBQ treatment. The level of FTL is strongly regulated by the level of labile iron (51,52), and an increase in FTL is an indicator of an elevation of labile iron (53). Meanwhile, a cell surface iron transporter ferroportin (Fpn) facilitating the export of cytosolic iron

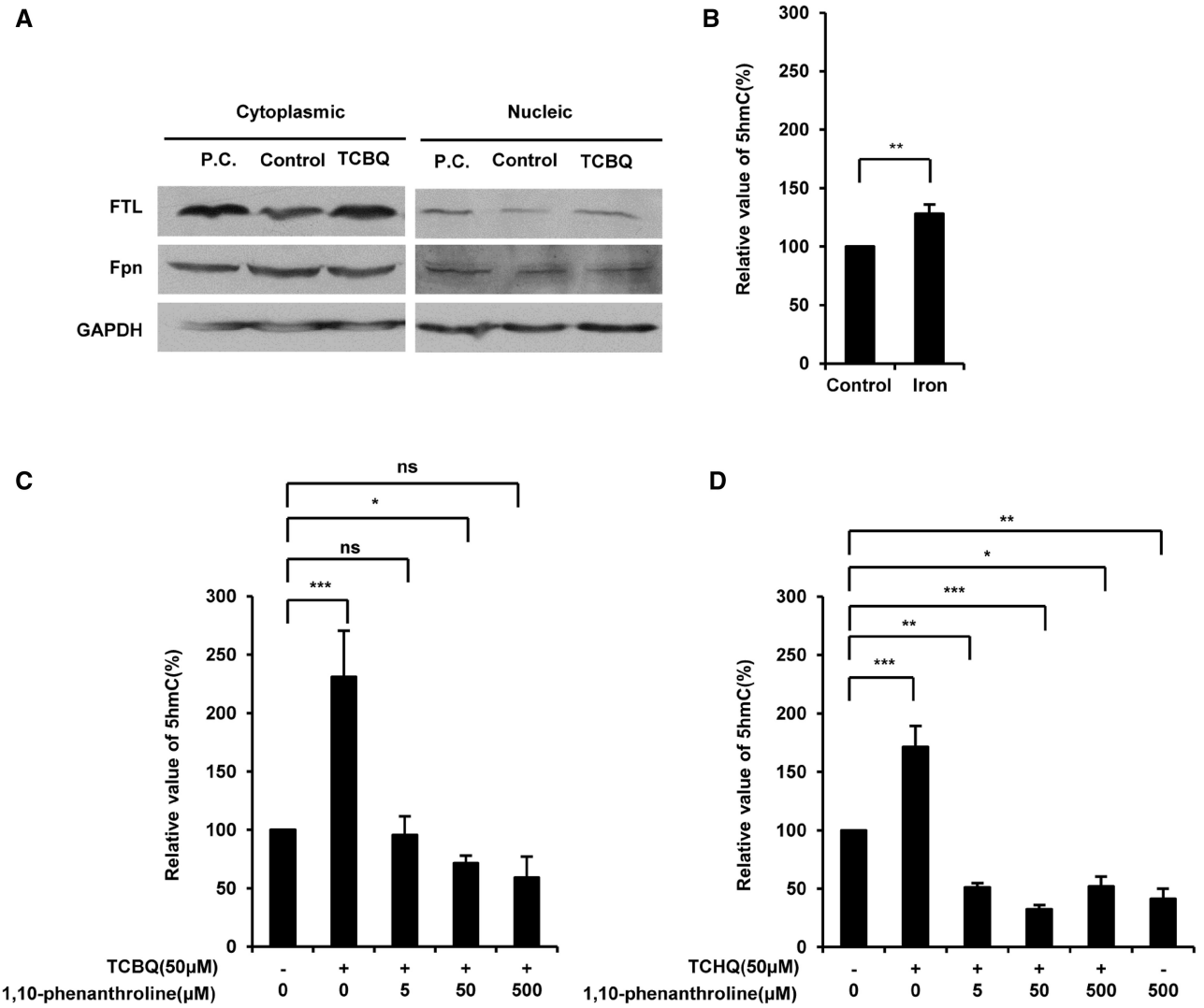

Figure 3. The quinone stimulation of Tet oxidation activity is associated with iron regulation *in vivo*. (**A**) Analysis of expression of ferritin light-chain (FTL) and ferroportin (Fpn) proteins within cytoplasmic and nucleic extracts of 20 μM TCBQ-treated MRC-5 cells. The extracts of 100 μM ferric nitrilotriacetate (Fe-NTA)-treated cells were applied for positive control (P.C.). Control protein was extracted from 0.02% (v/v) DMSO-treated cells. (**B**) Quantifications of 5hmC in genomic DNA from MRC-5 cells treated by 100 μM ammonium ferric citrate (FAC) for 12 h. Control genomic DNA was extracted from the cells treated with 0.1% (v/v) sterilized ddH_2O. (**C** and **D**) Quantifications of 5hmC in genomic DNA from A549 cells treated with 50 μM TCBQ (C) or TCHQ (D) in the absence or presence of 1,10-phenanthroline (0–500 μM). $^{*}P < 0.05$, $^{**}P < 0.01$, $^{***}P < 0.001$, $^{ns}P > 0.05$, determined using Student's *t*-test, two-tailed. Error bars, mean ± S.E.M. for triplicate experiments.

(53) was almost not influenced upon TCBQ treatment. These results indicated a higher level of cellular labile iron contributing to the stimulation of Tet oxidation activity by quinones. The increase in labile iron pool would supply more iron (II) to iron (II)- and α-ketoglutarate-dependent Tet proteins, by which the Tet-catalyzed reaction (5mC oxidation and 5hmC formation) could be enhanced. This further prompted us to investigate the role of iron availability in Tet-catalyzed reactions at cellular level.

We first delivered iron (II) to MRC-5 cells with an assistance of a weak chelator ammonium ferric citrate As a result of 12 h iron delivery, the level of 5hmC efficiently increased by 30% (Figure 3B). We then examined the role played by intracellular labile iron in the formation of 5hmC using 1,10-phenanthroline, a lipophilic and membrane-permeable iron-specific chelating agent (54). We found that 5hmC was reduced by this iron-chelating agent (5–500 μM) to the background level in TCBQ- or TCHQ-treated cells (Figure 3C and D), confirming the involvement of intracellular labile iron.

Generation of 5hmC in cells by other redox-active quinones

Interestingly, the generation of 5hmC in cellular DNA could also be promoted by a number of other quinoid compounds, including less halogenated quinones such as 2-chloro-1,4-benzoquinone (2-CBQ), 2,5-dichloro-1, 4-benzoquinone (2,5-DCBQ) and 2,6-dichloro-1,4-benzoquinone (2,6-DCBQ), and highly halogenated quinones, e.g., tetrabromo-1,4-benzoquinone (TBrBQ) and

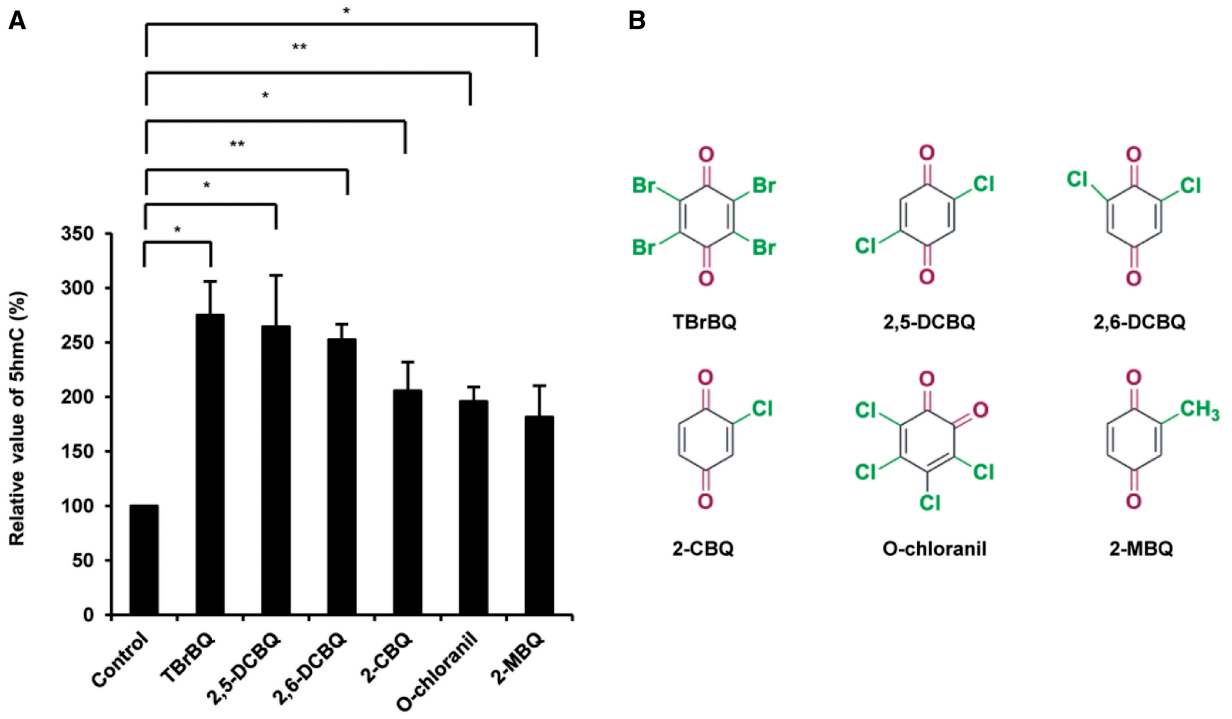

Figure 4. The levels of 5hmC in A549 cells treated with other redox active quinones. The tested quinones include tetrabromo-1,4-benzoquinone (TBrBQ), 2,5-dichloro-1,4-benzoquinone (2,5-DCBQ), 2,6-dichloro-1,4-benzoquinone (2,6-DCBQ), 2-chloro-1,4-benzoquinone (2-CBQ), O-chloranil and 2-methyl-1,4-benzoquinone (2-MBQ). $*P < 0.05$, $**P < 0.01$, determined using Student's *t*-test, two-tailed. Error bars, mean ± S.E.M. for triplicate experiments.

O-chloranil (Figure 4). In addition, the methylated quinones (e.g., 2-methyl-1,4-benzoquinone (2-MBQ)) also promoted 5hmC formation. As shown in Figure 4A, halogenated quinones had higher activities for the generation of 5hmC in cells compared to non-halogenated quinones, TBrBQ-treatment increased the level of 5hmC by ~2.8-fold compared to the control, and ~2.0-fold increase was observed upon O-chloranil treatment. However, even for the non-halogenated quinone, 2-MBQ, the level of 5hmC was also raised by ~1.8-fold compared to the DMSO control, which was comparable to the level of 5hmC in cells treated with TCBQ (~1.9-fold, Figure 1B). This indicates that a number of redox-active quinoid compounds have a strong ability to stimulate the conversion of 5mC to 5hmC in mammalian cells (Figure 4).

Genome-wide profile of 5hmC induced by TCBQ treatment

Quinones can be derived from many natural as well as synthetic chemical compounds and are therefore an inevitable part of the cellular environment (31). 5mC is an important epigenetic mark and our finding that quinones are capable of promoting the conversion of 5mC to 5hmC, thereby altering this mark, might have a wide range of biological consequences for the cell. To test the extension of this quinone-induced epigenetic change, we analyzed the genome-wide 5hmC distribution after quinone treatment by deep-sequencing of chemically labeled 5hmC (11). We found that the TCBQ-induced 5hmC is associated with gene-rich regions in MRC-5 cells (Figure 5A and B and Supplementary Table S1). We identified a total of 17 767 5hmC peaks in the genome of MRC-5 cells treated with TCBQ ($P < 10^{-5}$, fold change >5) among which 76.9% of the peaks were located within either intergenic regions (7324) or introns (6330). The remaining 5hmC peaks were found in exons (1117), 5′UTR (1081) and 3′UTR (651), respectively (Figure 5C and Supplementary Table S2). The 5hmC peaks that fall into either the gene bodies or up-/down-stream of the genes might regulate gene expression and were associated with 5751 genes. In contrast, we only identified 6976 5hmC peaks in the genome of control DMSO solvent treated MRC-5 cells (Figure 5C and Supplementary Table S2). Strikingly, following TCBQ treatment we observed a significant enrichment of 5hmC in gene bodies as well as in proximal upstream and downstream regions relative to TSSs and transcription end sites (TESs) (Figure 5D). Thus, these analyses demonstrate that TCBQ treatment induces genome-wide but not loci-specific 5hmC formation. In order to investigate the potential functions of 5hmC, we did KEGG pathway and GO term analysis of the 5751 genes, which revealed that these genes belong to various functional groups including protein catabolic process, phosphorylation, cell cycle, pathways in cancer, cellular transport, protein complex assembly, etc. (Supplementary Figure S4).

TCBQ regulates gene expression via 5hmC enrichment

To determine if TCBQ-induced 5hmC formation results in changes in gene expression, we took advantage of

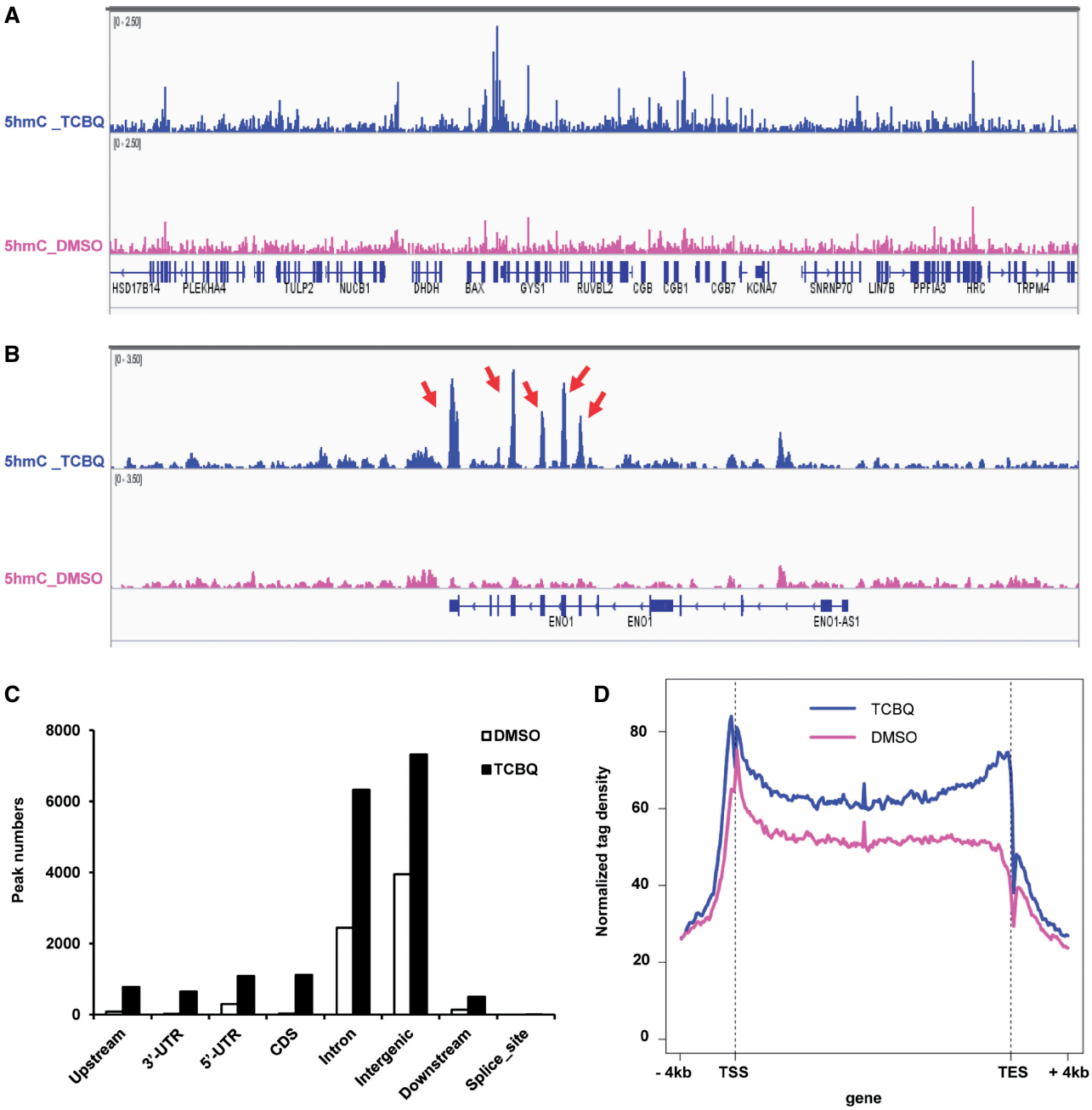

Figure 5. Genome-wide 5hmC formation by TCBQ treatment. (**A**) 5hmC densities in the region of chr19:49,319,120-49,696,264 of TCBQ treated (blue) and Control DMSO treated (pink) MRC-5 cell samples by 5hmC pull-down and deep sequencing. (**B**) 5hmC densities in the region of chr1:8,904,958-8,950,900 of TCBQ treated (blue) and Control DMSO treated (pink) MRC-5 cell samples by 5hmC pull-down, the red arrows indicate the TCBQ induced peaks. (**C**) 5hmC peak numbers of TCBQ treated (blue) and Control DMSO treated (pink) samples in different genomic regions ($P < 0.005$, fold change > 5). (**D**) Normalized 5hmC tag density distribution across the gene body. Each gene body was normalized to 0%–100%. Normalized Tag density is plotted from 4 kb upstream of TSSs to 4 kb downstream of TESs.

RNA-sequencing technology (RNA-Seq) to compare the transcriptomes of Control DMSO and TCBQ treated MRC-5 cells (Supplementary Table S3). We detected the expression of a total of 17 569 genes, with 10 484 genes showing a significant difference in expression by using DEGseq software in which genes with $P < 0.001$ and $q < 0.05$ were defined as differentially expressed genes (Figure 6A and Supplementary Table S6). We next asked whether this difference in gene expression was associated with 5hmC modification of the genes. Indeed, 3414 of the above 5751 genes enriching 5hmC show a significant difference in expression (Figure 6B). GO and enrichment analysis of these genes showed that TCBQ treatment resulted in 5hmC-mediated gene expression changes of genes belonging to several different functional groups, including protein catabolic process, apoptosis, protein localization and transport, protein complex assembly, RNA processing, phosphorylation, cell

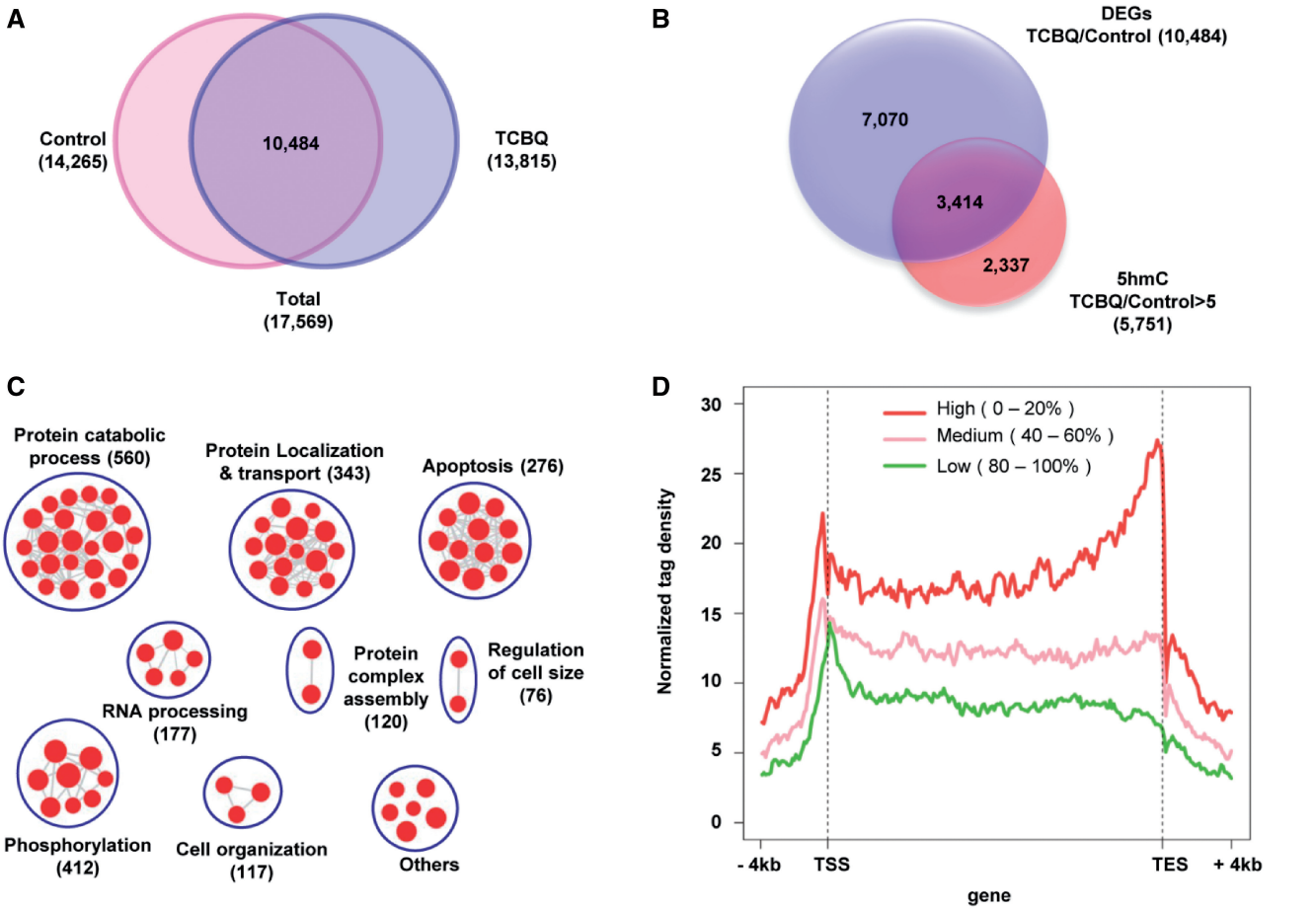

Figure 6. TCBQ regulates gene expression via increasing 5hmC enrichment. (**A**) Transcriptome analysis identified a total of 17 569 gene expressed in TCBQ and Control DMSO treated MRC-5 cells, and 10 484 of them are differentially expressed in TCBQ- compared to DMSO-treated cells (with the cutoff of RPKM ≥ 1, $P < 0.001$, $q < 0.05$). (**B**) Genes with peaks at which 5hmC is significantly increased (>5-fold change) and gene expression is significantly increased in gene bodies in TCBQ- compared to DMSO-treatment ($P < 0.001$, $q < 0.05$). (**C**) GO and enrichment analysis for genes at which 5hmC is significantly increased (>5-fold change) and gene expression is significantly increased in gene bodies in TCBQ treatment compared to DMSO treatment. Red nodes represent enriched GO pathways. Clusters of functionally related gene-sets were generated manually. The cutoff parameters for enrichment analysis with Cytoscape software are as follows: $P < 0.005$, FDR $q < 0.05$, overlap cutoff > 0.5. (**D**) Normalized 5hmC density distribution in genes with high, medium or low expression levels. Genes were sorted by expression levels from high to low and divided into five tiers. The first, third and fifth tier were selected to represent genes of high, medium and low expression, respectively.

organization, regulation of cell size and other regulatory pathways (Figure 6C). This suggests that quinone-dependent 5hmC generation could influence a broad range of cellular functions.

Metagene 5hmC read density profiles for RefSeq transcripts revealed that gene expression level correlated with both intragenic and proximal enrichment of 5hmC (Figure 6D), consistent with a role for 5hmC in maintaining and/or promoting gene expression (11). Among these genes, about 55% of the genes enriching 5hmC were down-regulated. The other 1523 of the above 3414 genes enriching 5hmC were up-regulated and selected for further enrichment analysis based on DAVID GO tool and visualized as an enrichment map using Cytoscape software (Figure 7A and Supplementary Figure S5A). A large proportion of these genes are related to protein catabolic process, apoptosis signaling pathway, cell localization and transport process, RNA processing procedures (Figure 7A). We further validated several genes which have increased levels in both 5hmC and gene expression by conventional RT-qPCR and BA combined with qPCR assays, respectively (Figure 7B and C; Supplementary Figure S5B and 5C; Supplementary Tables S4 and S5).

DISCUSSION

Here we demonstrate that redox-active chemicals stimulate oxidative conversion of 5mC to 5hmC in a TET dioxygenase-dependent manner. Redox-active quinones induce genome-wide 5hmC modifications affecting expression of thousands genes involved in a broad range of cellular processes. The conversion of 5mC to 5hmC has been linked to epigenetic reprogramming, dynamic DNA demethylation and regulation of tissue-specific gene

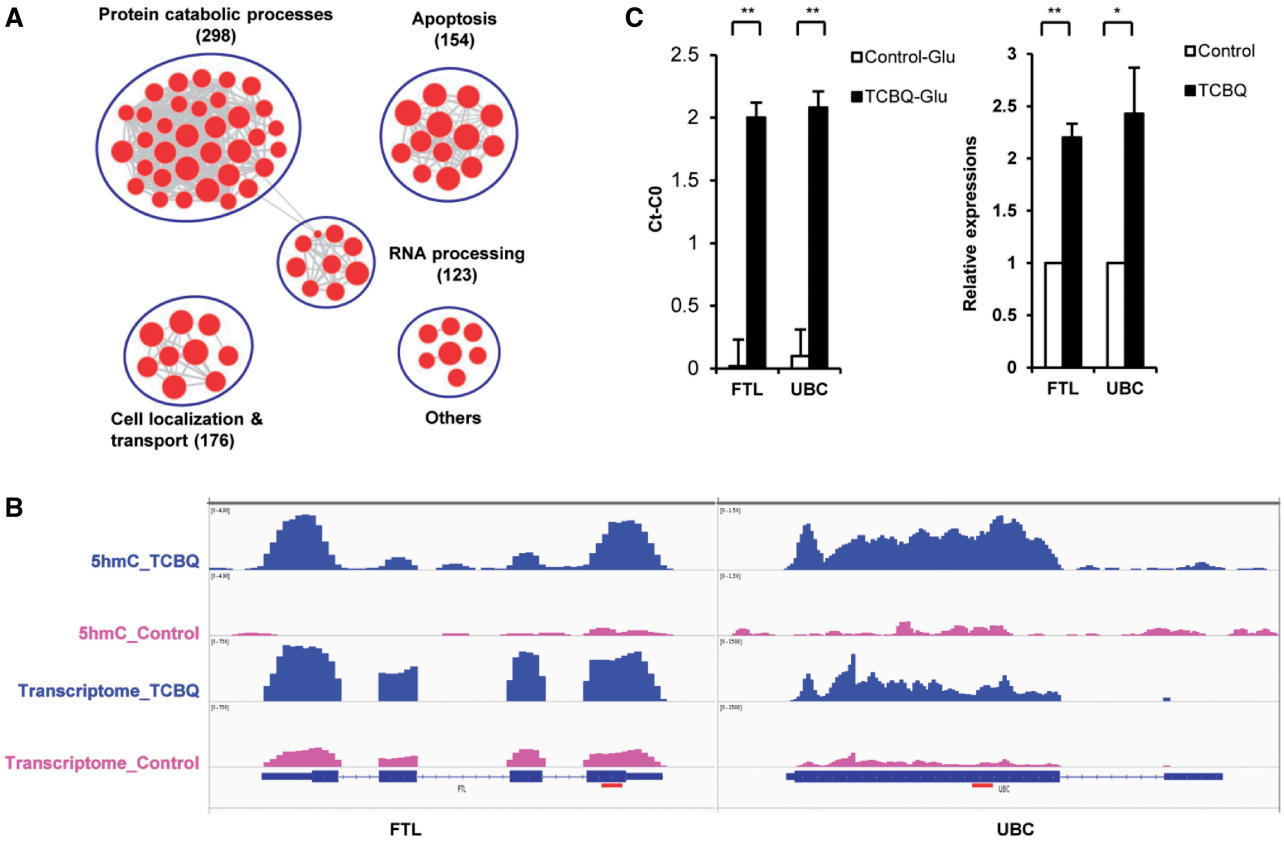

Figure 7. 5hmC enrichment induced by TCBQ treatment positively correlated to gene expression. (**A**) GO and enrichment analysis for the overlapped up-regulated genes is based on the DAVID GO result. The cutoff parameters for enrichment analysis with Cytoscape software are as follows: $P < 0.005$, FDR $q < 0.05$, overlap cutoff > 0.5. (**B**) Representative examples of individual genes and their values of 5hmC and gene expression from TCBQ treated (blue) and DMSO treated (pink) samples, FTL gene (left panel) and Ubiquitin C (UBC) gene (right panel) are shown here. (**C**) Verification of the 5hmC-enriched regions and expression of FTL gene (left panel) and UBC gene (right panel) by BA method combined with qPCR and RT-qPCR, respectively. The primer-targeted regions are noted by red lines in (B). $*P < 0.05$, $**P < 0.01$, determined using Student's *t*-test, two-tailed. Error bars, mean ± S.E.M. for triplicate experiments.

expression (55–57). Our data suggest that redox-active chemicals by inducing 5hmC formation could change the mammalian epigenome and hence affect various cellular processes. On the other hand, redox-active quinones can promote genome-wide DNA demethylation through enhancing genome-wide 5hmC formation as a result of Tet-mediated 5mC oxidation.

Aberrant 5hmC generation by quinones might very likely change the normal DNA methylation landscape, and thus alter the epigenetic control of gene expression. Genome-wide hypomethylation has been observed in cancer cells (58) and DNA demethylation mediated oncogene activation has been proposed to contribute to tumorigenesis (59). Furthermore, hypomethylation has been associated with genomic instability (60).

Interestingly, polychlorinated phenols, found in widely used biocides, generate redox-active halogenated quinones when metabolized and are under suspicion of being carcinogenic (41,61). We speculate that one cause of these biocides potential carcinogenicity could be their ability to convert 5mC to 5hmC in DNA. Finally, epigenetic manipulation by redox-active chemicals might aid in the development of new cancer therapies and regenerative medicine in the future.

ACCESSION NUMBERS

The GEO accession number for the deep-sequencing data reported in this article is GSE44457.

SUPPLEMENTARY DATA

Supplementary Data are available at NAR online.

ACKNOWLEDGEMENTS

Thanks to Dr. Sijin Liu for discussion and assistance in iron-regulation measurement at the Research Center for Eco-Environmental Sciences, Chinese Academy of Sciences.

FUNDING

973 programs [2010CB933502 to H.W, 2012CB518302 to Y.-G.Y., 2011YQ060084 to H.W.]; China Natural Science Foundation [21077129, 20877091, 20890112 and 21125523 to H.W., 31370796 to Y.-G.Y., 31250110215, 31150110143 to J.R.M.D.]. Funding for Open Access charge: [21077129].

Conflict of interest statement. None declared.

REFERENCES

1. Bird,A. (2002) DNA methylation patterns and epigenetic memory. *Genes Dev*., **16**, 6–21.
2. Ito,S., D'Alessio,A.C., Taranova,O.V., Hong,K., Sowers,L.C. and Zhang,Y. (2010) Role of Tet proteins in 5mC to 5hmC conversion, ES-cell self-renewal and inner cell mass specification. *Nature*, **466**, 1129–1133.
3. Kriaucionis,S. and Heintz,N. (2009) The nuclear DNA base 5-hydroxymethylcytosine is present in Purkinje neurons and the brain. *Science*, **324**, 929–930.
4. Tahiliani,M., Koh,K.P., Shen,Y., Pastor,W.A., Bandukwala,H., Brudno,Y., Agarwal,S., Lyer,L.M., Liu,D.R., Aravind,L. *et al.* (2009) Conversion of 5-methylcytosine to 5-hydroxymethylcytosine in mammalian DNA by MLL partner TET1. *Science*, **324**, 930–935.
5. He,Y.F., Li,B.Z., Li,Z., Liu,P., Wang,Y., Tang,Q., Ding,J., Jia,Y., Chen,Z., Li,L. *et al.* (2011) Tet-mediated formation of 5-carboxycytosine and its excision by TDG in mammalian DNA. *Science*, **333**, 1303–1307.
6. Ito,S., Shen,L., Dai,Q., Wu,S.C., Collins,L.B., Swenberg,J.A., He,C. and Zhang,Y. (2011) Tet proteins can convert 5-methylcytosine to 5-formylcytosine and 5-carboxylcytosine. *Science*, **333**, 1300–1303.
7. Globisch,D., Münzel,M., Müller,M., Michalakis,S., Wagner,M., Koch,S., Brückl,T., Biel,M. and Carell,T. (2010) Tissue distribution of 5-hydroxymethylcytosine and search for active demethylation intermediates. *PLoS One*, **5**, e15367.
8. Münzel,M., Globisch,D., Brückl,T., Wagner,M., Welzmiller,V., Michalakis,S., Müller,M., Biel,M. and Carell,T. (2010) Quantification of the sixth DNA base hydroxymethylcytosine in the brain. *Angew. Chem. Int. Ed*., **49**, 5375–5377.
9. Pastor,W.A., Pape,U.J., Huang,Y., Henderson,H.R., Lister,R., Ko,M., McLoughlin,E.M., Brudno,Y., Mahapatra,S., Kapranov,P. *et al.* (2011) Genome-wide mapping of 5-hydroxymethylcytosine in embryonic stem cells. *Nature*, **473**, 394–397.
10. Yu,M., Hon,G.C., Szulwach,K.E., Song,C.X., Zhang,L., Kim,A., Li,X., Dai,Q., Shen,Y., Park,B. *et al.* (2012) Base-resolution analysis of 5-hydroxymethylcytosine in the mammalian genome. *Cell*, **149**, 1368–1380.
11. Song,C.X., Szulwach,K.E., Fu,Y., Dai,Q., Yi,C., Li,X., Li,Y., Chen,C.H., Zhang,W., Jian,X. *et al.* (2011) Selective chemical labeling reveals genome-wide distribution of 5-hydroxymethylcytosine. *Nat. Biotechnol.*, **29**, 68–72.
12. Ko,M., Huang,Y., Jankowska,A.M., Pape,U.J., Tahiliani,M., Bandukwala,H.S., An,J., Lamperti,E.D., Koh,K.P., Ganetzky,R. *et al.* (2010) Impaired hydroxylation of 5-methylcytosine in myeloid cancers with mutant TET2. *Nature*, **468**, 839–843.
13. Langemeijer,S.M., Kuiper,R.P., Berends,M., Knops,R., Aslanyan,M.G., Massop,M., Linders,E.S., Hoogen,P., Kessel,A.G., Raymakers,R.A.P. *et al.* (2009) Acquired mutations in TET2 are common in myelodysplastic syndromes. *Nat. Genet*., **41**, 838–842.
14. Yin,R., Mao,S.Q., Zhao,B., Chong,Z., Yang,Y., Zhao,C., Zhang,D., Huang,H., Gao,J., Li,Z. *et al.* (2013) Ascorbic acid enhances Tet-mediated 5-methylcytosine oxidation and promotes DNA demethylation in mammals. *J. Am. Chem. Soc*., **135**, 10396–10403.
15. Baccarelli,A. and Bollati,V. (2009) Epigenetics and environmental chemicals. *Curr.Opin. Pediatr*., **21**, 243–251.
16. Skinner,M.K., Manikkam,M. and Guerrero-Bosagna,C. (2010) Epigenetic transgenerational actions of environmental factors in disease etiology. *Trends Endocrinol. Metabol*., **21**, 214–222.
17. Ho,S.M., Tang,W.Y., de Frausto,J.B. and Prins,G.S. (2006) Developmental exposure to estradiol and bisphenol A increases susceptibility to prostate carcinogenesis and epigenetically regulates phosphodiesterase type 4 variant. *Cancer Res*., **66**, 5624–5632.
18. Li,S., Hansman,R., Newbold,R., Davis,B., McLachlan,J.A. and Barrett,J.C. (2003) Neonatal diethylstilbestrol exposure induces persistent elevation of *c-fos* expression and hypomethylation in its exon-4 in mouse uterus. *Mol. Carcinog*., **38**, 78–84.
19. Huang,D., Zhang,Y., Qi,Y., Chen,C. and Ji,W. (2008) Global DNA hypomethylation, rather than reactive oxygen species (ROS), a potential facilitator of cadmium-stimulated K562 cell proliferation. *Toxicol. Letters*, **179**, 43–47.
20. Lee,Y.W., Klein,C.B., Kargacin,B., Salnikow,K., Kitahara,J., Dowjat,K., Zhitkovich,A., Christie,N.T. and Costa,M. (1995) Carcinogenic nickel silences gene expression by chromatin condensation and DNA methylation: a new model for epigenetic carcinogens. *Mol. Cell. Biol*., **15**, 2547–2557.
21. Kondo,K., Takahashi,Y., Hirose,Y., Nagao,T., Tsuyuguchi,M., Hashimoto,M., Ochiai,A., Monden,Y. and Tangoku,A. (2006) The reduced expression and aberrant methylation of $p16^{INK4a}$ in chromate workers with lung cancer. *Lung Cancer*, **53**, 295–302.
22. Dolinoy,D.C., Huang,D. and Jirtle,R.L. (2007) Maternal nutrient supplementation counteracts bisphenol A-induced DNA hypomethylation in early development. *Proc. Natl Acad. Sci. USA*, **104**, 13056–13061.
23. Rusiecki,J.A., Baccarelli,A., Bollati,V., Tarantini,L., Moore,L.E. and Bonefeld-Jorgensen,E.C. (2008) Global DNA hypomethylation is associated with high serum-persistent organic pollutants in Greenlandic Inuit. *Environ. Health Perspect*., **116**, 1547.
24. Wu,Q., Ohsako,S., Ishimura,R., Suzuki,J.S. and Tohyama,C. (2004) Exposure of mouse preimplantation embryos to 2, 3, 7, 8-tetrachlorodibenzo-p-dioxin (TCDD) alters the methylation status of imprinted genes H19 and Igf2. *Biol. Reprod*., **70**, 1790–1797.
25. Yang,X., Lay,F., Han,H. and Jones,P.A. (2010) Targeting DNA methylation for epigenetic therapy. *Trends Pharmacol. Sci*., **31**, 536–546.
26. Deb,S., Johnson,E.E., Robalinho-Teixeira,R.L. and Wessling-Resnick,M. (2009) Modulation of intracellular iron levels by oxidative stress implicates a novel role for iron in signal transduction. *Biometals*, **22**, 855–862.
27. Cairo,G., Tacchini,L., Pogliaghi,G., Anzon,E., Tomasi,A. and Bernelli-Zazzera,A. (1995) Induction of ferritin synthesis by oxidative stress transcriptional and post-transcriptional regulation by expansion of the "free" iron pool. *J. Bio. Chem*., **270**, 700–703.
28. Breuer,W., Epsztejn,S. and Ioav Cabantchik,Z. (1996) Dynamics of the cytosolic chelatable iron pool of K562 cells. *FEBS Lett*., **382**, 304–308.
29. Kakhlon,O. and Cabantchik,Z.I. (2002) The labile iron pool: characterization, measurement, and participation in cellular processes. *Free Rad. Biol. Med*., **33**, 1037–1046.
30. Wise,D.R., Ward,P.S., Shay,J.E., Cross,J.R., Gruber,J.J., Sachdeva,U.M., Platt,J.M., DeMatteo,R.G., Simon,M.C. and Thompson,C.B. (2011) Hypoxia promotes isocitrate dehydrogenase-dependent carboxylation of α-ketoglutarate to citrate to support cell growth and viability. *Proc. Natl Acad. Sci. USA*, **108**, 19611–19616.
31. Bolton,J.L., Trush,M.A., Penning,T.M., Dryhurst,G. and Monks,T.J. (2000) Role of quinones in toxicology. *Chem. Res. Toxicol*., **13**, 135–160.
32. Ravanat,J.L., Douki,T., Duez,P., Gremaud,E., Herbert,K., Hofer,T., Lasserre,L., Saint-Pierre,C., Favier,A. and Cadet,J. (2002) Cellular background level of 8-oxo-7,8-dihydro-2′-deoxyguanosine: an isotope based method to evaluate artefactual oxidation of DNA during its extraction and subsequent work-up. *Carcinogenesis*, **23**, 1911–1918.
33. Li,H. and Durbin,R. (2009) Fast and accurate short read alignment with Burrows-Wheeler transform. *Bioinformatics*, **25**, 1754–1760.
34. Zhang,Y., Liu,T., Meyer,C.A., Eeckhoute,J., Johnson,D.S., Bernstein,B.E., Nusbaum,C., Myers,R.M., Brown,M., Li,W. *et al.* (2008) Model-based analysis of ChIP-Seq (MACS). *Genome Biol*., **9**, R137.
35. Li,H. and Durbin,R. (2010) Fast and accurate long-read alignment with Burrows-Wheeler transform. *Bioinformatics*, **26**, 589–595.
36. Zhao,W., Liu,W., Tian,D., Tang,B., Wang,Y., Yu,C., Li,R., Ling,Y., Wu,J., Song,S. *et al.* (2011) wapRNA: a web-based application for the processing of RNA sequences. *Bioinformatics*, **27**, 3076–3077.

37. Mortazavi,A., Williams,B.A., McCue,K., Schaeffer,L. and Wold,B. (2008) Mapping and quantifying mammalian transcriptomes by RNA-Seq. *Nat. Methods*, **5**, 621–628.
38. Wang,L., Feng,Z., Wang,X., Wang,X. and Zhang,X. (2010) DEGseq: an R package for identifying differentially expressed genes from RNA-seq data. *Bioinformatics*, **26**, 136–138.
39. Benjamini,Y. and Hochberg,Y. (1995) Controlling the false discovery rate: a practical and powerful approach to multiple testing. *J. R. Stat. Soc. Ser. B*, **57**, 289–300.
40. Storey,J. and Tibshirani,R. (2003) Statistical significance for genomewide studies. *Proc. Natl Acad. Sci. USA*, **100**, 9440–9445.
41. Zhu,B.Z., Kalyanaraman,B. and Jiang,G.B. (2007) Molecular mechanism for metal-independent production of hydroxyl radicals by hydrogen peroxide and halogenated quinones. *Proc. Natl Acad. Sci. USA*, **104**, 17575–17578.
42. Zhu,B.Z. and Shan,G.Q. (2009) Potential mechanism for pentachlorophenol-inducedcarcinogenicity: A novel mechanism for metal-independent production of hydroxyl radicals. *Chem. Res. Toxicol.*, **22**, 969–977.
43. IARC Working Group. (1998) Re-evaluation of some organic chemicals, hydrazine and hydrogen peroxide. In: IARC Monographs on the Evaluation of Carcinogenic Risks to Humans. *Int. Agency Res. Cancer*, **71**, 61–63.
44. Qin,F., Zhao,Y.Y., Zhao,Y., Boyd,J.M., Zhou,W. and Li,X.F. (2010) A toxic disinfection by-product, 2, 6-dichloro-1, 4-benzoquinone, identified in drinking water. *Agnew. Chem. Int. Ed.*, **49**, 790–792.
45. Rao,K.R. (ed.), (1987) *Pentachlorophenol: Chemistry, Pharmacology, and Environmental Toxicology*. Plenum Press, New York, New York.
46. Reigner,B.G., Rigod,J.F. and Tozer,T.N. (1992) Disposition, bioavailability, and serum protein binding of pentachlorophenol in the B6C3F1 mouse. *Pharmacol. Res.*, **9**, 1053–1057.
47. Bass,D.A., Parce,J.W., Dechatelet,L.R., Szejda,P., Seeds,M.C. and Thomas,M. (1983) Flow cytometric studies of oxidative product formation by neutrophils: a graded response to membrane stimulation. *J. Immunol.*, **130**, 1910–1917.
48. Bienvenu,C., Wagner,J.R. and Cadet,J. (1996) Photosensitized oxidation of 5-methyl-2′-deoxycytidine by 2-methyl-1, 4-naphthoquinone: characterization of 5-(Hydroperoxymethyl)-2′-deoxycytidine and Stable Methyl Group Oxidation Products. *J. Am. Chem. Soc.*, **118**, 11406–11411.
49. Cao,H. and Wang,Y. (2007) Quantification of oxidative single-base and intrastrand cross-link lesions in unmethylated and CpG-methylated DNA induced by Fenton-type reagents. *Nucleic Acids Res.*, **35**, 4833–4844.
50. Jaakkola,P., Mole,D.R., Tian,Y.M., Wilson,M.I., Gielbert,J., Gaskell,S.J., Kriegsheim,A., Hebestreit,H.F., Mukherji,M., Schofield,C.J. *et al.* (2001) Targeting of HIF-α to the von Hippel-Lindau ubiquitylation complex by O_2-regulated prolyl hydroxylation. *Science*, **292**, 468–472.
51. Walden,W.E., Selezneva,A.I., Dupuy,J., Volbeda,A., Fontecilla-Camps,J.C., Theil,E.C. and Volz,K. (2006) Structure of dual function iron regulatory protein 1 complexed with ferritin IRE-RNA. *Science*, **314**, 1903–1908.
52. Mackenzie,E.L., Iwasaki,K. and Tsuji,Y. (2008) Intracellular iron transport and storage: from molecular mechanisms to health implications. *Antioxid. Redox Signal.*, **10**, 997–1030.
53. Nemeth,E., Tuttle,M.S., Powelson,J., Vaughn,M.B., Donovan,A., Ward,D.M., Ganz,T. and Kaplan,J. (2004) Hepcidin regulates cellular iron efflux by binding to ferroportin and inducing its internalization. *Science*, **306**, 2090–2093.
54. Imlay,J.A., Chin,S.M. and Linn,S. (1988) Toxic DNA damage by hydrogen peroxide through the Fenton reaction in vivo and in vitro. *Science*, **240**, 640–642.
55. Branco,M.R., Ficz,G. and Reik,W. (2011) Uncovering the role of 5-hydroxymethylcytosine in the epigenome. *Nat. Rev. Genet.*, **13**, 7–13.
56. Wu,H. and Zhang,Y. (2011) Mechanisms and functions of Tet protein-mediated 5-methylcytosine oxidation. *Genes Dev.*, **25**, 2463–2452.
57. Bhutani,N., Burns,D.M. and Blau,H.M. (2011) DNA demethylation dynamics. *Cell*, **146**, 866–872.
58. Feinberg,A.P. and Vogelstein,B. (1983) Hypomethylation distinguishes genes of some human cancers from their normal counterparts. *Nature*, **301**, 89–92.
59. Zhou,H., Chen,W.D., Qin,X., Lee,K., Liu,L., Markowitz,S.D. and Gerson,S.L. (2001) MMTV promoter hypomethylation is linked to spontaneous and MNU associated c-neu expression and mammary carcinogenesis in MMTV c-neu transgenic mice. *Oncogene*, **20**, 6009–6017.
60. Almeida,A., Kokalj-Vokac,N., Lefrancois,D., Viegas-Pequignot,E., Jeanpierre,M., Dutrillaux,B. and Malfoy,B. (1993) Hypomethylation of classical satellite DNA and chromosome instability in lymphoblastoid cell lines. *Hum. Genet.*, **91**, 538–546.
61. Yin,R., Zhang,D., Song,Y., Zhu,B.Z. and Wang,H. (2013) Potent DNA damage by polyhalogenated quinones and H_2O_2 via a metal-independent and intercalation-enhanced oxidation mechanism. *Scientific Rep.*, **3**, 1269.